Multi-parametric MRI for Contrast Agent Free Breast DCE-MRI Synthesis

Zhikai Yang[1], Cristina Zhang[1], Huijian Chen[2], Muzhen He[2], and Rodrigo Moreno[1]

1 Dept. of Biomedical Engineering and Health Systems, KTH Royal Institute of Technology
Stockholm, Sweden
2 Dept. of Radiology,Shengli Clinical Medical College of Fujian Medical University & Fujian Provincial Hospital & Fuzhou University Affiliated Provincial Hospital
Fuzhou, China
zhikai@kth.se, rodmore@kth.se

Abstract. Dynamic contrast-enhanced Magnetic Resonance Imaging (DCE-MRI) is a critical tool for breast cancer detection and diagnosis. Yet, its reliance on contrast agents presents risks, increases cost, and is contraindicated for certain patients, necessitating a contrast-agent-free alternative. In this paper, we use a conditional Generative Adversarial Network (GAN) with a multi-scale enhancement consistency loss for contrast agent-free breast DCE-MRI synthesis from a multi-parametric MRI input (T1w, multi-b-value DWI, and ADC maps) The proposed loss explicitly enforces consistency of the predicted enhancement maps across multiple scales. The model generates multiple DCE post-contrast phases simultaneously, reducing inference time and computational overhead. The proposed framework achieved the best performance among previous methods on public and in-house datasets. The code is available at https://github.com/minnelab/DCE-MRI-Syn.

Keywords: DCE-MRI, Contrast Synthesis, GANs, Deep Learning

1 Introduction

Breast cancer is the most common cancer in women. Magnetic resonance imaging (MRI) offers the highest sensitivity for breast cancer detection. Particularly, dynamic contrast-enhanced MRI (DCE-MRI) can delineate tumors well and has become indispensable for detection and diagnosis. However, numerous studies have reported that gadolinium-based contrast agents (GBCAs) can cause allergic and other adverse reactions. In addition, GBCA injection increases both cost and examination time [14, 17]. Consequently, acquiring contrast-enhanced information without contrast agents has become an important research direction.

Deep learning based method have become a promising solution for DCE-MRI synthesis. For DCE-MRI synthesis, most previous studies have only used structural MRI (T1-weighted (T1w) or T2-weighted (T2w) images) [14, 11, 17,

12, 13]. However, studies have shown that multi-parametric MRI using T1w, T2w, Diffusion-Weighted Imaging (DWI), Proton Density (PD), and Apparent Diffusion Coefficient (ADC) yields better estimates than using only T1w as the input [2, 3, 16, 9].

Several studies have used deep learning to generate contrast-enhanced images from low-dose contrast or non-contrast agent images [5, 14, 11, 17, 12, 13]. Most of these methods are based on Convolution Neural Network (CNNs) [16, 5, 14], diffusion-based models [9, 10, 4, 6, 13], and Generative Adversarial Networks (GANs) [17, 11–13], Diffusion models may achieve better results but at a cost of longer training and inference times, making them less suitable for clinical settings. Within GANs, attention-based models are usually the most accurate [7, 15, 2]. Multi-parametric MRI image synthesis uses different MRI sequences as the input. The different MRI sequences offer tissue properties, giving complementary useful information for image synthesis. However, there are only a few studies (e.g., [16]) that have used multi-parametric MRI for virtual contrast enhancement synthesis, incorporating DWI and ADC maps for breast DCE-MRI synthesis, despite their rich diagnostic information.

Motivated by this, we develop a conditional generative model that leverages T1w MRI together with multi-b-value DWI and ADC as inputs to synthesize DCE-MRI. Our contributions are summarized as follows:

- We propose a method with multi-parametric conditional input to synthesize the multiple post-phases in Breast DCE-MRI.
- A Multi-Scale Enhancement Consistency (MSEC) module is introduced to improve virtual contrast enhancement detail structure.
- We tested the method on public and private datasets were used to validate its generalizability.

2 Method

Fig. 1 summarizes the proposed method. The input is a pre-contrast T1-weighted image, the ADC map, and diffusion-weighted images acquired at different b-values. The architecture is based on the Pix2PixHD framework [18], consisting of a generator G and two discriminators D_i to capture global and local features. Unlike existing approaches that generate a single post-contrast phase, our method generates multiple post-phases simultaneously with a single model.

The generator processes inputs at both full and half resolutions to balance global structural consistency and fine-texture detail. The two discriminators are designed as a multi-scale PatchGAN: (i) D_1 operates on full-resolution images to capture local texture and edge fidelity, and (ii) D_2 operates on downsampled images to ensure global structural realism across scales.

The total loss function is a weighted combination of four components:

$$\mathcal{L}_{\text{GAN}} = \lambda_{\text{adv}}\, \mathcal{L}^{\text{D}}_{\text{adv}} + \lambda_{\text{fm}}\, \mathcal{L}^{\text{D}}_{\text{fm}} + \lambda_{\text{per}}\, \mathcal{L}_{\text{per}} + \lambda_{\text{sub-ms}} \mathcal{L}_{\text{sub-ms}}, \tag{1}$$

where $\mathcal{L}^{D}_{\text{adv}}$ denotes the least-squares adversarial (LSGAN) losses from the two discriminators (full resolution / downsampled), $\mathcal{L}^{D}_{\text{fm}}$ denote the feature-matching

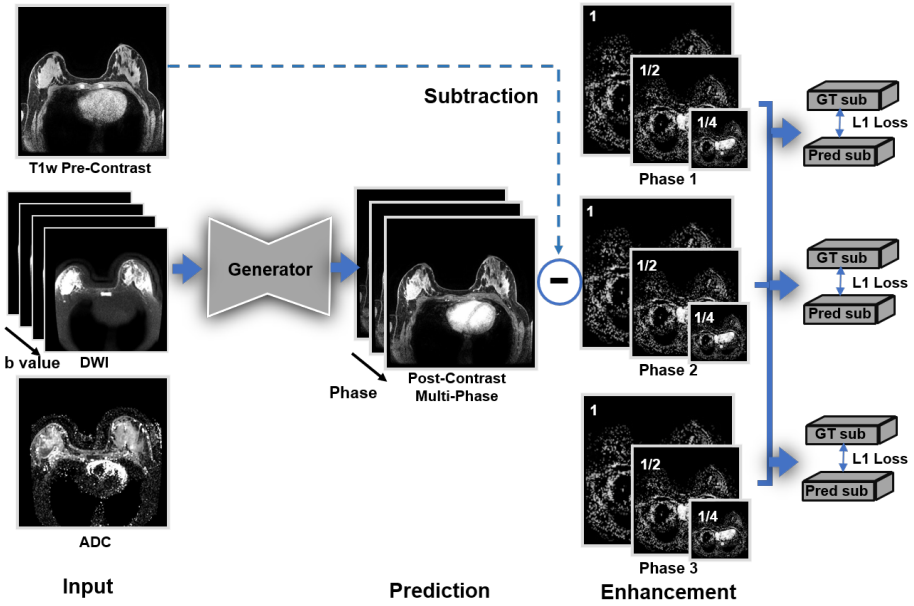

Fig. 1. Overview of the proposed multiple sequence DCE-MRI synthesis method. The proposed method is based on the GANs framework with a multiscale subtraction consistency method incorporated with T1w, DWI, and ADC.

losses computed from intermediate discriminator features, $\mathcal{L}_{\text{per}}$ denotes the perceptual loss that preserves high-level semantic consistency, and $\mathcal{L}_{\text{sub-ms}}$ denotes the proposed multi-scale subtraction loss, which enforces consistency of the predicted enhancement map across different image levels. The hyperparameters λ_{adv}, λ_{fm}, λ_{per} and $\lambda_{\text{sub-ms}}$ control the relative contributions of these terms.

Multi-Scale Enhancement Consistency: The goal of the MSEC loss is to help the prediction be coherent at both global and local image levels. To explicitly model the post-contrast enhancement process, we define an enhancement map as $s_k = y_k - x_0$, where x_0 denotes the pre-contrast image and y_k denotes the k-th post-contrast phase. The generator first predicts $\hat{s}_k$ and reconstructs the synthesized post-contrast image as $\hat{y}_k = x_0 + \hat{s}_k$.

During training, for each phase k we estimate $s_k = y_k - x_0, \hat{s}_k = \hat{y}_k - x_0$. Notice that negative values of s_k are not physically possible. Then, we define the MSEC loss as:

$$\mathcal{L}_{\text{ms-sub}} = \sum_{r \in \{1, \frac{1}{2}, \frac{1}{4}\}} \sum_{k} \left\| \text{down}_r(\hat{s}_k) - \text{down}_r(s_k) \right\|_1 \tag{2}$$

where down$(\cdot)$ is the downsampling operator. Thus, the MSEC loss considers L_1 losses at three different downsampling levels. For comparison, we also tested the same approach with a single scale (SSEC) in the experiments.

The key advantage of MSEC loss is that it focuses on learning the true phase enhancement relative to x_0 rather than the absolute intensity, thereby enhancing dynamics and suppressing background, thereby improving sensitivity to low-contrast lesions and reducing under-/over-enhancement, improving cross-domain robustness and structural clarity. This loss term was set to $\lambda_{\mathrm{ms-sub}} = 50$ in our experiments. The model is trained for 150 epochs with the Adam optimizer. The learning rate is 2×10^{-4} that decays linearly from epoch 100.

3 Experimental Results

Dataset: The public dataset used in this study is from the ACRIN-6698/I-SPY2 breast MRI trial on The Cancer Imaging Archive, used in the BMMR2 challenge [8]. All MRI examinations were performed on 1.5T or 3.0T systems with a dedicated breast radiofrequency (RF) coil, with patients in the prone position; longitudinal exams for each patient were acquired on the same scanner configuration. The protocol included T1w DCE-MRI with a phase duration of 80–100 s where 5 post-contrast enhanced phases were acquired; and DWI using a 4-*b*-value scheme (b = 0, 100, 600, 800 s/mm^2). Furthermore, an additional in-house dataset from Fuzhou University [19] was used for external validation, including 27 patients acquired by 3T scanner (MAGNETOM Prisma,Siemens Healthcare, Erlangen, Germany). This dataset has DCE-MRI with 36 post-contrast phases with 30 second interval and 9 DWI with b-values (b = 0, 30, 50, 80, 120, 160, 200, 500, 1000 s/mm^2). From them, we selected $b = 0$, 80, 500, 1000 s/mm^2, which are the closest to the ones of BMMR2.
Preprocessing: We selected post-contrast phases 1, 3, and 5 from the BMMR2 dataset for training and validation. For the in-house dataset, for each patient, we selected three similar acquisition time phases for testing. For each image, we extracted the axial central slice, along with 5 superior and 5 inferior slices (including a proportion of non-tumor slices to enhance diversity). Each 2D axial slice intensities were linearly scaled between the 1st and 99th percentiles to [0,1] and resized to 512×512 with bilinear interpolation. The dataset is split 90% for training and 10% for validation at the subject level, with a fixed random seed of 42 for reproducibility. In total, the dataset comprises 4790 and 710 2D slices per modality for training and validation, respectively.

3.1 Evaluation Protocol

The root mean square error (RMSE), Peak Signal-to-Noise Ratio (PSNR), and Structure Similarity Index Measure (SSIM) were used for quantitative evaluation. We compare the baseline Pix2PixHD method with different inputs and variants of our methods. Furthermore, we also compared the results with other representative contrast enhancement generation methods, including an attention-based method (AAD) [2] and a diffusion-based method [6]. The AAD method used the ADC and T1w as input; for the diffusion-based method, we use the T1w, ADC, and DWI sequence input for fair comparison. Furthermore, we also perform ablations to assess the different components of the method.

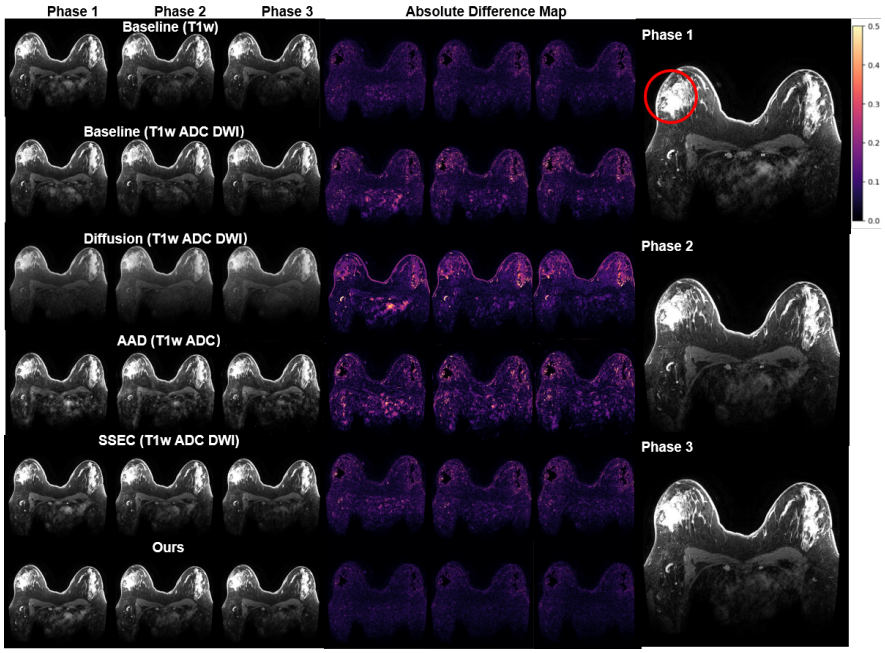

Fig. 2. Visualization of synthesis results and error maps for different methods at the BMMR2 dataset. Left: Synthesized different phases of images using different methods. Middle: absolute difference maps at different phases ($\|GT - Pred\|$). Right: Post-contrast image ground truth (the red circle indicates the lesion region).

3.2 Qualitative Evaluation

Fig. 2 displays phases 1-3 and absolute difference maps of one case. It can be observed that: (1) Compared to other methods, ours preserves sharper cortical and vascular details across all three phases, with crisper lesion boundaries. (2) The error map indicate lower overall error in parenchyma and substantially reduced high-frequency error along lesion margins, suggesting better structural consistency. (3) When conditioned only on T1w, methods without the multi-scale consistency and multi-parameter fusion tend to over-smooth textures.

Fig. 3 shows contrast-enhancement curves in the lesion for a representative case from BMMR2. Across phases, our method enhancement is consistently closer to the ground truth, particularly at Phase 2 (contrast rising) and Phase 3 (plateau), indicating a more faithful recovery of enhancement dynamics.

Since the DCE-MRI most important region is the lesion region, Fig.4 compares different methods' contrast enhancement curves within the lesion ROI across the entire BMMR2 testing set. The result shows that the proposed method has the most similar trend to the ground truth and a smaller error.

Additionally, to validate the generalization performance, we compared the different methods on the in-house dataset at different phases, which was not used

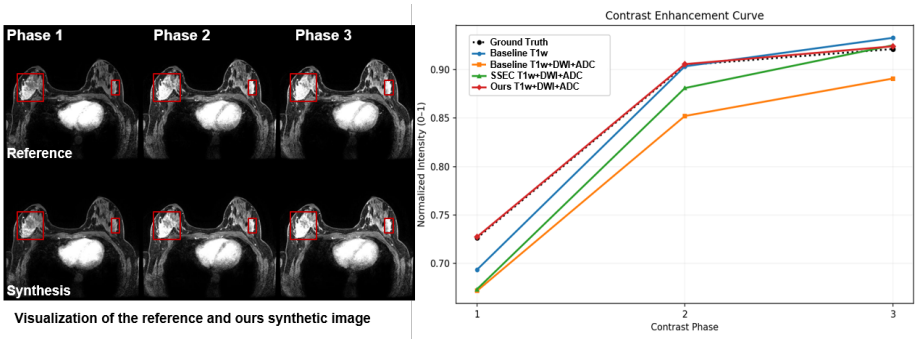

Fig. 3. Comparison of different components of contrast enhancement curves in the lesion region of the representative image from the BMMR2 dataset. Left: visualization of reference and synthesized images with our method. Right: comparison of contrast enhancement curves with different methods.

Table 1. Comparison of different methods with different inputs.

Dataset	Method	PSNR ↑	SSIM ↑	RMSE ↓
BMMR2	Baseline (T1w)	21.720	0.699	0.081
	Baseline (T1w ADC DWI)	20.490	0.650	0.102
	AAD (T1w ADC)	21.020	0.638	0.091
	Diffusion (T1w ADC DWI)	19.600	0.677	0.210
	SSEC (T1w ADC DWI)	22.280	0.690	0.087
	MSEC (T1w)	24.970	0.781	0.070
	MSEC (T1w ADC)	25.140	0.780	0.069
	MSEC (T1w DWI)	25.032	0.781	0.069
	Ours	**25.370**	**0.783**	**0.068**
In-house	AAD (T1w ADC)	12.31	0.310	0.244
	Diffusion (T1w ADC DWI)	16.73	**0.593**	0.296
	Ours	**18.29**	0.553	**0.123**

for training shown in Fig.5. Qualitatively, the proposed method has the best and closest visual quality compared to ground truth, especially in the lesion region, which has distinct enhancement. AAD has the worst generalization performance, and the diffusion-based method could produce some detail region but it shows lower contrast enhancement than ours.

3.3 Quantitative Evaluation

Table 1 summarizes the quantitative evaluation of methods. We compare the BMMR2 testing set and in-house dataset at the baseline Pix2Pix model with different inputs and other representative methods. As shown, our method outperforms previous methods and baselines. It shows our method has a significant difference in all metrics across all the evaluated methods using the Friedman

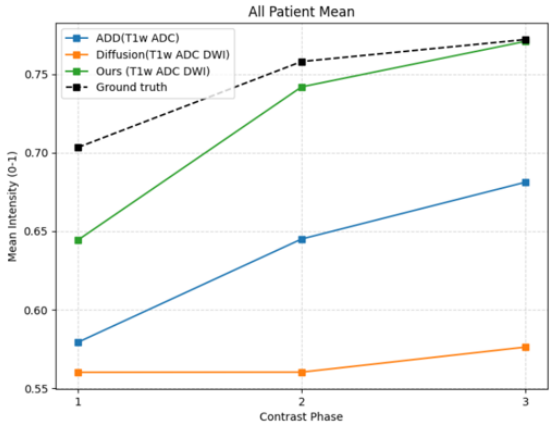

Fig. 4. Mean enhancement curves for the different methods on the testing set of the BMMR2 dataset in lesion regions.

Table 2. Phase-wise RMSE within the lesion ROI.

Dataset	Method	Phase 1	Phase 2	Phase 3	Overall
BMMR2	AAD (T1w ADC)	0.124	0.112	0.091	0.109
	Diffusion (T1w ADC DWI)	0.143	0.197	0.195	0.178
	Ours	**0.058**	**0.016**	**0.001**	**0.025**
In-house	AAD (T1w ADC)	0.372	0.338	0.287	0.333
	Diffusion (T1w ADC DWI)	0.301	0.335	0.311	0.315
	Ours	**0.167**	**0.143**	**0.098**	**0.136**

test, followed by post-hoc analysis using the Nemenyi test ($p < 0.05$). The table also shows that our method benefits from using multiparametric MRI inputs and the MSEC loss. As expected, all methods have a drop in performance in the in-house dataset compared to the BMMR2 dataset, as it was not used for training and with different acquisition protocol. However, our method still has the best PSNR and RMSE with a moderate SSIM score. The diffusion-based method has the best SSIM score for the in-house dataset. But our method achieves the best PSNR and RMSE.

Additionally, Table 2 shows the RMSE per phase within the lesions for both datasets. In all cases, our method outperforms AAD and the diffusion method. Notice that the performance increases in Phase 3, suggesting improved robustness to late-phase enhancement and residual background noise.

4 Conclusion

In this work, we present a deep learning based multi-parametric MRI-based virtual contrast enhancement synthesis method. To improve the synthesis image

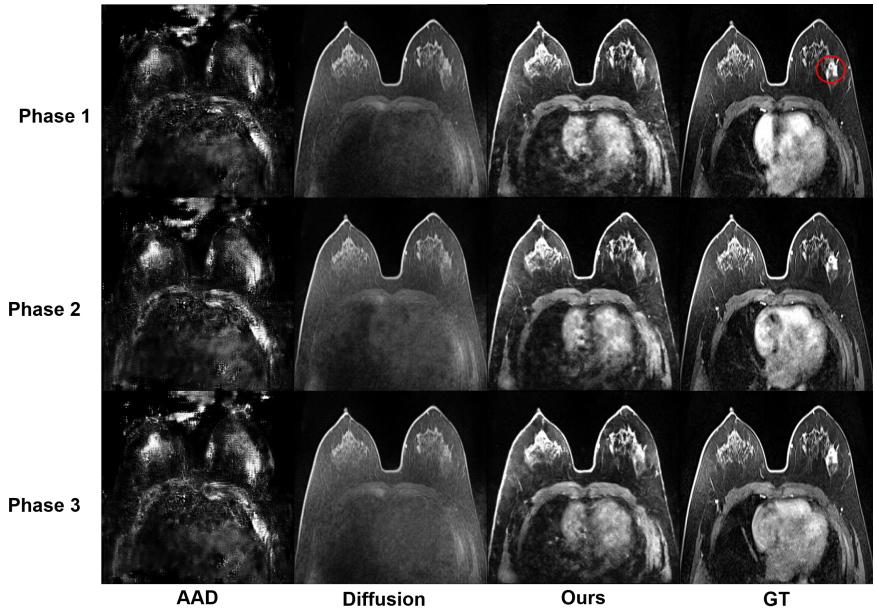

Fig. 5. Visualization of our method's DCE-MRI synthesis results compared to the ground truth in one subject of the in-house dataset. Red circle indicates the lesion.

quality, we proposed a multi-scale enhancement consistency loss for improving the detailed structure of image quality. Compared with solely structure-based MRI images, our method produces the closest synthetic contrast-enhanced image to the ground-truth DCE-MRI among existing synthesis methods. Additionally, the use of multi-parametric MRI improved accuracy. While T1w could provide the anatomical information, ADC and DWI can provide prior information for estimating perfusion information. The method generalized well using an external clinical dataset.

We acknowledge the limitations of the proposed methods. Due to data availability, we now only incorporate the DWI, ADC, and T1w for synthesis. Other types of contrast-free modalities could also contribute to increased performance. Since we only focus on dynamic enhancement of the breast region, in future work, we will use segmentation to make the generation only focus on enhancement changes in that region. Moreover, we will explore the generation of more phases and harmonization mechanisms to re-standardize the acquisition time of every phase across subjects. In summary, we presented a contrast-free, multi-phase DCE synthesis framework leveraging ADC and multi-b DWI conditioning to synthesize the post-contrast DCE-MRI. The proposed multi-scale enhancement consistency loss yields the best image quality and fidelity, and mitigates false enhancement. From a clinical perspective, the proposed model generates contrast-enhanced-like multi-phase DCE-MRI directly from non-contrast MRI,

potentially reducing risks, costs, and scan time, while expanding accessibility for patients contraindicated for GBCA use.

Disclosure of Interests. The authors have no competing interests to declare.

Acknowledgment. This work was supported by grants from Marie Skłodowska-Curie Doctoral Networks Actions (HORIZON-MSCA-2021-DN-01-01; 101073222), Cancerfonden (22-2389 Pj), STINT (CH2019-8301, CH2020-8710), and Natural Science Foundation of Fujian Province, China (2024J011643, to Muzhen He). In addition to the use of MAIA [1], we thank the Knut and Alice Wallenberg Foundation and the National Academic Infrastructure for Supercomputing in Sweden for the use of Berzelius and Alvis, which is partially funded by the Swedish Research Council (grant 2022-06725).

References

1. Bendazzoli, S., Persson, S., Astaraki, M., Pettersson, S., Grozman, V., Moreno, R.: MAIA: a collaborative medical AI platform for integrated healthcare innovation. npj Artificial Intelligence **1**(1), 45 (2025)
2. Bharti, D., Ramanarayanan, S., Ram, K., Agarwal, H., Venkatesan, R., Sivaprakasam, M., et al.: AAD-DCE: An aggregated multimodal attention mechanism for early and late dynamic contrast enhanced prostate MRI synthesis. In: IEEE International Conference on Acoustics, Speech and Signal Processing (ICASSP). pp. 1–5. IEEE (2025)
3. Chen, C., Raymond, C., Speier, W., Jin, X., Cloughesy, T.F., Enzmann, D., Ellingson, B.M., Arnold, C.W.: Synthesizing MR image contrast enhancement using 3D high-resolution ConvNets. IEEE Transactions on Biomedical Engineering **70**(2), 401–412 (2022)
4. Fan, X., Xu, L., Zheng, B., Zeng, X., Li, W., Huang, Z.: Pre-to post-contrast medical image synthesis with outline-guide accelerate diffusion model. Neural Networks p. 107851 (2025)
5. Gong, E., Pauly, J.M., Wintermark, M., Zaharchuk, G.: Deep learning enables reduced gadolinium dose for contrast-enhanced brain MRI. Journal of Magnetic Resonance Imaging **48**(2), 330–340 (2018)
6. Ibarra, S., del Riego, J., Catanese, A., Cuba, J., Cardona, J., Leon, N., Infante, J., Lekadir, K., Diaz, O., Osuala, R.: Comparing conditional diffusion models for synthesizing contrast-enhanced breast MRI from pre-contrast images. In: Deep Breast Workshop on AI and Imaging for Diagnostic and Treatment Challenges in Breast Care. pp. 226–236. Springer (2025)
7. Jin, Y., Lin, G., Yang, Q., Chen, Z., Liu, H., Wang, B., Zhang, N., Zheng, H., Liang, D., Luo, D., et al.: Pixel-level transformer GAN for enhanced parametric mapping of DCE MRI analysis. Medical Physics **52**(9), e18092 (2025)
8. Li, W., Partridge, S.C., Newitt, D.C., Steingrimsson, J., Marques, H.S., Bolan, P.J., Hirano, M., Bearce, B.A., Kalpathy-Cramer, J., Boss, M.A., et al.: Breast multiparametric MRI for prediction of neoadjuvant chemotherapy response in breast cancer: the BMMR2 challenge. Radiology: Imaging Cancer **6**(1), e230033 (2024)

9. M, K.K., Ramanarayanan, S., S, S., Sarkar, A., Gayathri, M.N., Ram, K., Sivaprakasam, M.: DCE-diff: Diffusion model for synthesis of early and late dynamic contrast-enhanced MR images from non-contrast multimodal inputs. In: Proceedings of the IEEE/CVF Conference on Computer Vision and Pattern Recognition (CVPR) Workshops. pp. 5174–5183 (2024)
10. Müller-Franzes, G., Huck, L., Bode, M., Nebelung, S., Kuhl, C., Truhn, D., Lemainque, T.: Diffusion probabilistic versus generative adversarial models to reduce contrast agent dose in breast MRI. European Radiology Experimental **8**(1), 53 (2024)
11. Osuala, R., Joshi, S., Tsirikoglou, A., Garrucho, L., Pinaya, W.H., Diaz, O., Lekadir, K.: Pre-to post-contrast breast MRI synthesis for enhanced tumour segmentation. In: SPIE Medical Imaging: Image Processing. vol. 12926, pp. 226–237 (2024)
12. Osuala, R., Joshi, S., Tsirikoglou, A., Garrucho, L., Pinaya, W.H., Lang, D.M., Schnabel, J.A., Diaz, O., Lekadir, K.: Simulating dynamic tumor contrast enhancement in breast MRI using conditional generative adversarial networks. Journal of Medical Imaging **12**(S2), S22014–S22014 (2025)
13. Osuala, R., Lang, D.M., Verma, P., Joshi, S., Tsirikoglou, A., Skorupko, G., Kushibar, K., Garrucho, L., Pinaya, W.H., Diaz, O., et al.: Towards learning contrast kinetics with multi-condition latent diffusion models. In: International Conference on Medical Image Computing and Computer-Assisted Intervention (MICCAI). pp. 713–723. Springer (2024)
14. Preetha, C.J., Meredig, H., Brugnara, G., Mahmutoglu, M.A., Foltyn, M., Isensee, F., Kessler, T., Pflüger, I., Schell, M., Neuberger, U., et al.: Deep-learning-based synthesis of post-contrast T1-weighted MRI for tumour response assessment in neuro-oncology: a multicentre, retrospective cohort study. The Lancet Digital Health **3**(12), e784–e794 (2021)
15. Sadhana, S., Ramanarayanan, S., Sarkar, A., Ram, K., Gayathri, M.N., Joel, S., Agarwal, H., Venkatesan, R., Sivaprakasam, M.: DCE-former: A transformer-based model with mutual information and frequency-based loss functions for early and late response prediction in prostate DCE-MRI. In: IEEE International Symposium on Biomedical Imaging (ISBI). pp. 1–5 (2024)
16. Schreiter, H., Eberle, J., Kapsner, L.A., Hadler, D., Ohlmeyer, S., Erber, R., Emons, J., Laun, F.B., Uder, M., Wenkel, E., et al.: Virtual dynamic contrast enhanced breast MRI using 2D U-Net architectures. In: Deep Breast Workshop on AI and Imaging for Diagnostic and Treatment Challenges in Breast Care. pp. 85–95. Springer (2024)
17. Wang, P., Nie, P., Dang, Y., Wang, L., Zhu, K., Wang, H., Wang, J., Liu, R., Ren, J., Feng, J., et al.: Synthesizing the first phase of dynamic sequences of breast MRI for enhanced lesion identification. Frontiers in Oncology **11**, 792516 (2021)
18. Wang, T.C., Liu, M.Y., Zhu, J.Y., Tao, A., Kautz, J., Catanzaro, B.: High-resolution image synthesis and semantic manipulation with conditional GANs. In: IEEE Conference on Computer Vision and Pattern Recognition (CVPR) (2018)
19. Zhang, H., Zheng, Y., Zhang, M., Wang, A., Song, Y., Wang, C., Yang, G., Ma, M., He, M.: Breast cancer: Habitat imaging based on intravoxel incoherent motion for predicting pathologic complete response to neoadjuvant chemotherapy. Medical Physics (2025)